SCIENTIFIC REPORTS

OPEN

SUBJECT AREAS:
ENDOPLASMIC RETICULUM
PROTEIN AGGREGATION
PROTEIN TRANSPORT
STRUCTURAL BIOLOGY

Received
28 May 2013

Accepted
20 August 2013

Published
16 September 2013

Correspondence and requests for materials should be addressed to S.B. (bonatti@unina.it) or M.S. (mariano.stornaiuolo@gmail.com)

A disorder-to-order structural transition in the COOH-tail of Fz4 determines misfolding of the L501fsX533-Fz4 mutant

Valentina Lemma[1], Massimo D'Agostino[1], Maria Gabriella Caporaso[1], Massimo Mallardo[1], Giorgia Oliviero[2], Mariano Stornaiuolo[1] & Stefano Bonatti[1]

[1]Department of Molecular Medicine and Medical Biotechnology, University of Naples Federico II, 80131 Naples, Italy, [2]Department of Pharmacy, University of Naples Federico II, 80131 Naples, Italy.

Frizzled 4 belongs to the superfamily of G protein coupled receptors. The unstructured cytosolic tail of the receptor is essential for its activity. The mutation L501fsX533 in the *fz*4 gene results in a new COOH-tail of the receptor and causes a form of Familial exudative vitreoretinopathy. Here we show that the mutated tail is structured. Two amphipathic helices, displaying affinity for membranes and resembling the structure of Influenza Hemagglutinin fusion peptide, constitute the new fold. This tail induces the aggregation of the receptor in the Endoplasmic Reticulum and it is sufficient to block the export to the Golgi of a chimeric VSVG protein containing the mutated tail. Affecting the tail's structure, net charge or amphipathicity relocates the mutated Fz4 receptor to the Plasma Membrane. Such disorder-to-order structural transition was never described in GPCRs and opens a new scenario on the possible effect of mutations on unstructured regions of proteins.

The correct activity of a protein relies on its tridimensional fold. Functionality is achieved when each domain of a protein acquires the right structural conformation. Similarly, disordered regions need to remain as such. Genetic mutations (substitution, deletion and insertion) alter the primary sequence of a protein and may interfere with the acquisition of a specific conformation or dictate a new fold. The intracellular destiny of the protein and its activity depends on the effect of these mutations. The protein may remain active, less active or, more dramatically, a misfolded unfunctional protein may be generated. Many examples of the effect of genetic mutations on the structured regions of a protein are described[1]. Despite recent evidence suggesting that a considerable percentage of mutations fall in disordered domains of proteins[2], little is known on the outcome of such amino acid substitutions in these disordered parts. Disordered regions are enriched in short linear motives that serve as binding site for other proteins and such interaction are crucial for cell signaling[3,4]. Structural disorder can be defined by the number of conformations that a protein domain can acquire due to its structural freedom. Intrinsic disordered regions have been associated with particular cellular functions including cell regulation, DNA-protein interaction and ligand binding[5–8]. Disordered regions do not always stay unstructured but can acquire a fold after they interact with intracellular partners or with ligands and cofactors[9]. Mutations may abolish these structural transitions interfering either with the recognition of the partner or with the structural transition itself[10].

Frizzled4 (Fz4) belongs to the family of Frizzled cell surface receptors that are involved in a variety of biological processes during development as well as in adult life[11,12]. Fz4 displays the structural landmarks observed in G protein-coupled receptors[11,12]: an ectosolic N-Terminus, seven hydrophobic transmembrane segments, three intracellular and extracellular loops and a cytosolic C-terminal tail[13]. Two PDZ binding motives are located one internally and one at the C-terminus of Fz4. The cytosolic tail of Fz4 has been shown to interact with the protein Dishevelled to activate several signalling pathways[14–16]. The frameshift mutation L501fsX533 of Fz4 is associated with a rare form of Familial exudative vitreorethinopaty (FEVR)[17] that shows an autosomal dominant inheritance. The mutation generates a different and shorter C-terminal cytosolic tail. The resulting mutant receptor (henceforth referred as Fz4-FEVR) fails to reach the Plasma Mambrane (PM) of the cells and accumulates in the Endoplasmic Reticulum (ER)[17,18]. It has been suggested that this mutant would trap wild type chains by improper heteroligomerization, thus abolishing Fz4 signaling from the cell surface during retinal development by a dominant negative mechanism[18]. This loss

of function results in an aberrant vascularization of the retina during development with severe consequences for the patients[19,20].

Here we show that the frameshift mutation generates a disorder-to-order structural transition in the tail of Fz4-FEVR. The new tail acquires a helix-loop-helix fold and its conformation structurally resembles the fusion peptide of Influenza Hemagglutinin at the pH of fusion[21]. We prove that the new tail is amphipathic and displays affinity for membranes, a feature that hampers the folding of Fz4 and results in the formation of covalent disulfide-linked aggregates. The effect of the Fz4-FEVR tail is not only exerted in the context of Fz4 folding. A chimera composed by ectodomain and transmembrane regions of the reporter molecule Vesicular Stomatitis Virus Glycoprotein (VSVG) fused to the cytosolic tail of Fz4-FEVR is trapped in the ER in a prefolded state. Shape and curvature of the tail is proven essential for membrane interaction both in the cell and *in vitro*. We finally prove that shifting the fold of Fz4-FEVR tail back to a more disordered conformation or affecting its net charge or amphipathicity by mutation of key residues rescues the localization of the mutant receptor to the PM.

Results

Fz4-FEVR protein accumulates in the ER as a misfolded aggregate. Fz4 wt, transiently expressed in Huh-7 cells, localizes at the PM as shown by immunofluorescence staining performed on unpermeabilized cells (Fig. 1a). Intracellularly, Fz4 localizes mainly in a perinuclear region of the cells corresponding to the Golgi complex (Fig. 1c). In contrast, Fz4-FEVR does not appear on the PM (Fig. 1b) and shows a clear ER localization (Fig. 1d), as shown by double labeling with the ER marker calnexin (Fig. 1e and f). The same results were obtained in HEK-293 and COS-7 cells (data not shown). Comparison of the mobility on SDS-PAGE of the reduced proteins showed the absence of the mature form in Fz4-FEVR, while the analysis of not reduced samples indicated that this mutant generates almost exclusively inter and intra chain S-S linked covalent aggregates (Fig. 1g), most likely the cause of its trapping in the ER. To further prove the ER localization of Fz4-FEVR, the Endo-H sensitivity of the protein was tested in a pulse-chase assay. Fz4 and Fz4-FEVR were transiently expressed in HEK 293 cells and both resulted sensitive to Endo H treatment immediately after the

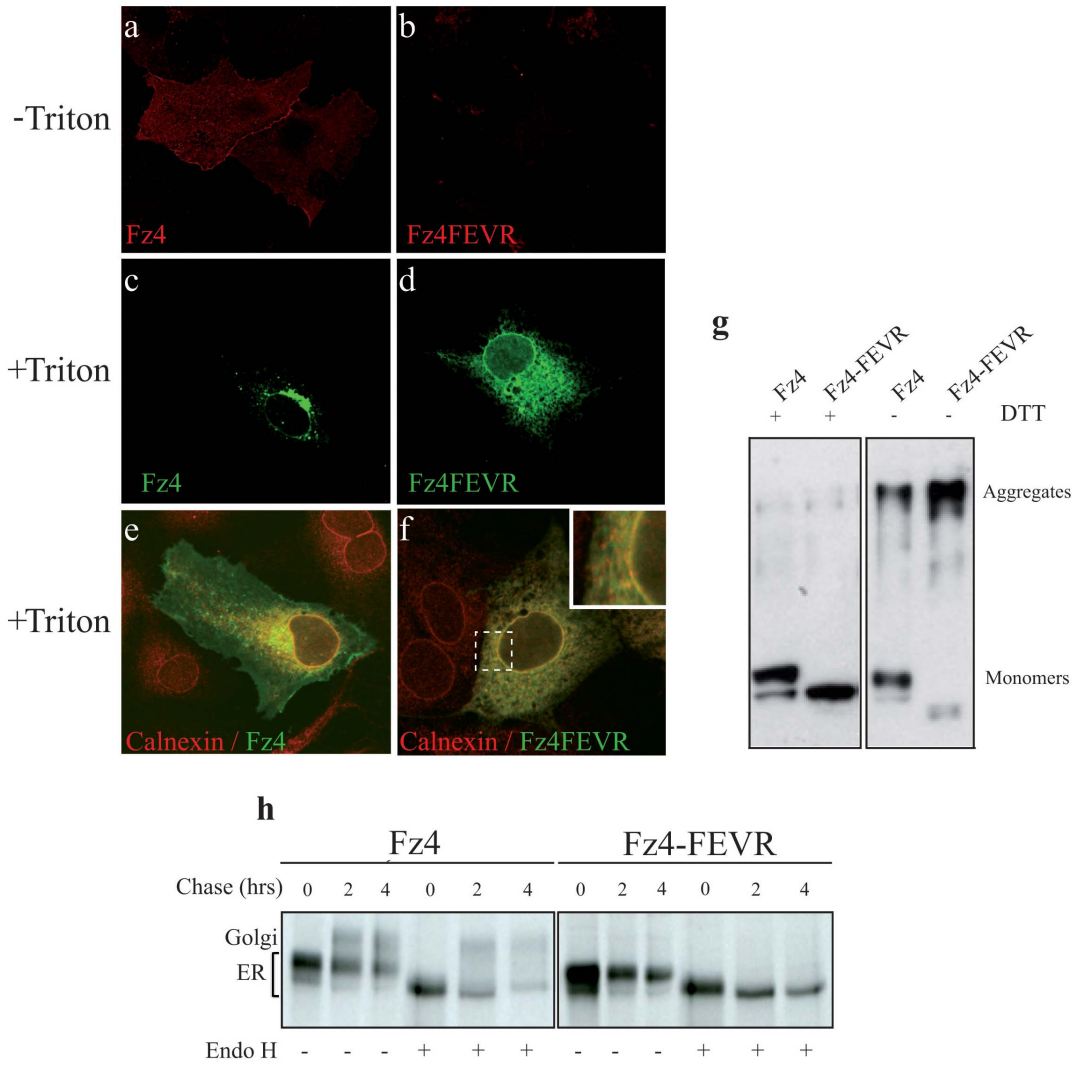

Figure 1 | Fz4-FEVR fails to reach the Plasma Membrane and aggregates in the Endoplasmatic Reticulum. Surface (−Triton) and intracellular (+Triton) localization of Fz4 (a, c) and Fz4-FEVR (b, d) and their colocalization with the ER marker Calnexin (e–f) after transient transfection in Huh-7 cells. The inset in f shows in yellow region of colocalization; g) SDS-PAGE analysis of Fz4 and Fz4-FEVR run in reducing (+DTT) and not-reducing conditions (−DTT) (reduced and non reduced samples have been run under the same experimental conditions; monomeric and aggregated forms are indicated, only relevant parts of the gels are shown); (h) Endo-H resistance (Golgi) and sensitivity (ER) of newly synthesised Fz4 and Fz4-FEVR chains pulse-chase labelled for the indicated time after transient transfection in HEK 293 cells (only relevant parts of the gels are shown; samples have been run under the same experimental conditions).

pulse (Fig. 1h). After 2 and 4 hours of chase, an Endo H resistant band appeared for Fz4 but not for Fz4-FEVR, thus confirming that only the wild type protein reaches the Golgi complex and acquires the sugar modifications responsible for the resistance (Fig. 1h). Moreover, a proteomic-based approach aimed at the identification of specific interactors of Fz4-FEVR tail did not suggest proteins that could explain the ER retention of the mutant receptor[22]. Taken together, these results show that the new tail of Fz4-FEVR hampers the folding of the receptor causing its misfolding and retention in the ER.

Prediction of the Fz4-FEVR tail fold. Fz4-FEVR has a different and shorter C-terminal cytosolic tail (Fig. 2a). Search in protein databases found no similarity between the aminoacidic sequence of the Fz4-FEVR tail (Fig. 2b) and any other sequence. Surprisingly, structure prediction softwares (see Materials and Methods for details) suggested the Fz4-FEVR tail to be folded (Fig. 2b). The prediction indicates the mutated tail to acquire a helix-loop-helix conformation. Two consecutive helices (helix 1 Ser_{501} to Gly_{516} and helix 2 Lys_{523} to Lys_{530}), connected by a six amino acids long loop (Lys_{517} to Arg_{522}) define the predicted fold (Fig. 2b). The loop is predicted for the structural similarity with helix-loop-helix containing proteins like transcription factors and calcium binding proteins [PDB: 1R9D[23], 3FGH[24], 1GT0[25]]. Charged side chains like the ones present in the Fz4-FEVR loop (Lys_{517}, $Asp_{518,\ 520,\ 521}$ and $Arg_{519,\ 522}$) are common in helix connecting loops and are responsible for the curvature, due to their interaction with water molecules or with ions[26]. The same prediction softwares suggested only a small helical region for the juxtamenbrane portion of the C-terminal tail of the wt receptor (Lys_{499} to Arg_{510}) (Fig. 2b). The existence of this short helix has already been postulated and shown to be involved in the interaction of Fz4 with the effector protein Dishevelled[15,27], while the remaining part of the wt tail (from Leu_{511} to Val_{537}) was predicted to be disordered[27]. We judged the structure prediction for the mutant tail sound and worthwhile of further experimental proof.

Conformation of the Fz4-FEVR tail in solution. To confirm the predicted fold, a synthetic peptide corresponding to the Fz4-FEVR tail was analyzed by Circular Dichroism (CD)[28]. The spectrum was compared with that of a synthetic Fz4 wt tail and of a modified Fz4-FEVR mutant in which part of the loop sequence between amino acid R_{519} and W_{524} was replaced by 6 Alanine residues (Fz4-FEVR-6Ala), thus conferring more flexibility to the Fz4-FEVR tail (Fig. 2b). Indeed, the CD spectrum of the Fz4-FEVR tail peptide showed two negative picks at around 208 and 222 nm, proper of an helical fold with a molar ellipticity ratio Θ[222 nm]/Θ[208 nm] proximum to 1[28] (Fig. 2d). The CD spectrum of the wt tail peptide also showed two negative picks at almost the same wavelengths. However, the ratio Θ[222 nm]/Θ[208 nm] was less than 1. The decrease of molar ellipticity ratio usually reflects the contribution of other fold (for random coil minimum at 198 nm and maximum in the 210–230 nm region) to the average spectrum[28]. This would indicate that the Fz4 tail peptide is less structured, as expected[28]. The ratio Θ[222 nm]/Θ[208 nm] in the Fz4-FEVR-6Ala CD spectrum was lower than one, confirming to be more disordered than the Fz4-FEVR tail peptide(Fig. 2d). Therefore, the CD analysis indicated that a synthetic peptide corresponding to the sequence of Fz4-FEVR tail acquires a stable alpha-helical conformation in solution, confirming the structural prediction. In contrast, the synthetic Fz4-wt and Fz4-FEVR-6Ala tail peptides appeared more flexible in solution. Since Fz4-FEVR-6Ala misses the loop region of the Fz4-FEVR tail (R_{519}-W_{524}), it is likely that this loop causes the structural stability of the Fz4-FEVR tail fold.

Affinity of Fz4-FEVR tail for membranes. According to the structural prediction, the two helices of the Fz4-FEVR peptide have a boomerang shape forming a planar angle of about 90° (Ala_{504}-Lys_{517}-Lys_{530}) and a dihedral angle of 23° (Ala_{504}-Lys_{517}-Arg_{522}-Lys_{530}) (Supplementary Fig. S1a, b). Hydrophobic and aromatic residues all face the inner side of the boomerang making the Fz4-FEVR structure strongly amphipathic (Fig. 3a and Supplementary Fig. S1c). In contrast, a more random distribution of polar and non polar amino acids is predicted for the not structured wt tail. The flexibility of the C-terminal parts of both Fz4 and Fz4-FEVR-6Ala does not make them amphipathic (Fig. 3a). While structure based similarity searches indicate structural homology to transcription factors, we noticed that Fz4-FEVR tail resembles in shape and hydrophobicity the fusion peptide of HA at the pH of fusion [PDB 1IBN[21]] [root mean square (r.m.s.) deviation on alpha carbons 1.075 Å] (Supplementary Fig. S1). The structural alignment between HA fusion peptide with Fz4 wt tail indicates only poor similarity (r.m.s. score of 1.373 Å). The boomerang shape formed by the two consecutive helices of HA fusion peptide (102° planar angle and 35° dihedral angle) (Supplementary Fig. S1a, b) was shown to be essential to enable the fusion of the viral peptide to the membrane and mutation even marginally affecting the shape of the fold resulted in peptides with less fusogenic activity[29,30]. Thus, the similarity of Fz4-FEVR tail to HA fusion peptide and its amphipathicity would suggest affinity for membranes. In the context of the full length Fz4-FEVR protein, an interaction of this tail with the membrane is likely, due to the close proximity of the tail to the lipid bilayer of the cytosolic side of the ER.

To test the affinity of the Fz4-FEVR tail for the membranes, the CD spectra of the peptides were recorded in the presence of a micellar agent, the non ionic detergent ANAPOE-$C_{10}E_6$[31] (Fig. 3b). This detergent is endowed of spectral properties not interfering with most of the structural biology assays. In the presence of micelles, the Θ at 222 and 208 nm of the Fz4-FEVR tail peptide increased four times, proving the peptide has affinity for membranes and that its fold gets stabilized by the lipids. The ratio Θ[222 nm]/Θ[208 nm] was almost unchanged, suggesting a neutral effect of the micelles on the structure of the peptide. A minimal effect was visible when the micellar agent was added to the wt peptide, suggesting a much minor propensity of this sequence to interact with the micelles. Surprisingly, ANAPOE-$C_{10}E_6$ modified the CD spectrum of Fz4-FEVR-6Ala peptide. A clear increase of Θ at 208 and 222 nm was recorded and the ratio Θ[222 nm]/Θ[208 nm] went closer to 1, suggesting that despite its flexibility in solution the peptide can acquire a more stable alpha-helical fold in the presence of membranes (Fig. 3b). In contact with the micelles the stability of Fz4-FEVR peptide drastically increases as shown by the raise in the melting temperature of the peptide in the presence of the micelles (Fig. 3c). Thus, the CD spectra indicated that the helical regions Ser_{501} to Gly_{516} and Lys_{523} to Lys_{530} (present in both Fz4-FEVR and in Fz4-FEVR-6Ala peptides) have affinity for membranes that in turn stabilize the helical fold. In the absence of membranes the loop region R_{519} and W_{524} of the Fz4-FEVR tail probably stabilizes the helix-loop-helix conformation of the tail.

To further prove the interaction of Fz4-FEVR and Fz4-FEVR-6Ala tails with membranes, we measured changes in Trp fluorescence intensity and Trp fluorescence polarization[32] in the presence of micelles (Fig. 3d, e). Fz4-FEVR has one Trp located on helix 1 and two on helix 2. Trp fluorescence was measured in the presence of increasing concentration of ANAPOE-$C_{10}E_6$. In the presence of this detergent, a 2.2 fold increase in Trp fluorescence was measured suggesting a reduction in the number of the quenching water molecules around the Trp residues and consistent with an interaction of the peptide with the micelles. The increase in fluorescence is not visible at detergent concentration lower than the critical micellar concentration (c.m.c), confirming the need of formed micelles for the peptide to interact. Despite its affinity for membrane, a lower fluorescence increase was measured for the Fz4-FEVR-6Ala peptide above c.m.c.,

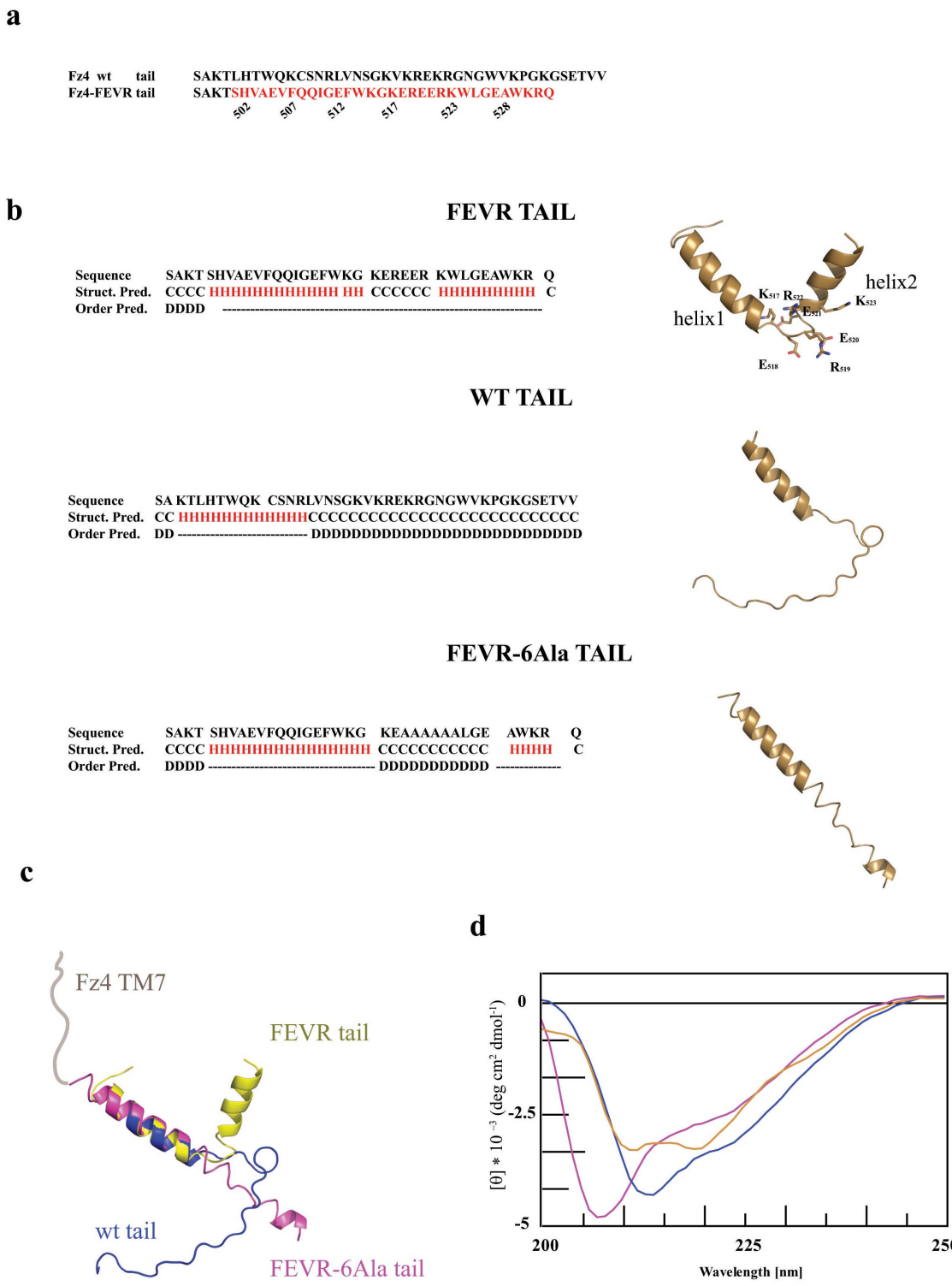

Figure 2 | Fz4 and Fz4-FEVR tails have a different fold. (a) Comparison of the amino acidic sequences of Fz4 wt and Fz4-FEVR C-terminal tails (numbering is referring to the mutant tail); (b) Structural prediction of Fz4wt, Fz4-FEVR and Fz4-FEVR-6Ala tails (C: coil; H: helix; D: disordered region; –: ordered region) and cartoon representation of the predicted structures. Residues contributing to the loop of Fz4-FEVR tail are shown in ball and sticks; (c) Superposition of the structural predictions of Fz4 wt, Fz4-FEVR and Fz4-FEVR-6Ala tails (cartoon blue, yellow and magenta, respectively). The gray line represents the seventh transmembrane segment of the Fz4 protein; (d) Superposition of the CD spectra of Fz4 wt, Fz4-FEVR and Fz4-FEVR-6Ala tails (colors as in (c)).

probably because it bears a single Trp residue or because the peptide is interacting differently with membrane (Fig. 3d).

Consistently with these results, an eight fold increase in Trp fluorescence polarization was measured for Fz4-FEVR tail at detergent concentration higher than the c.m.c. (Fig. 3e), suggesting a reduction in the speed of tumbling of the peptide in presence of the detergent and thus confirming its interaction with the micelles. No increase was measured for the Fz4-FEVR-6Ala peptide, a finding supporting that this tail has a different way of insertion in the membrane.

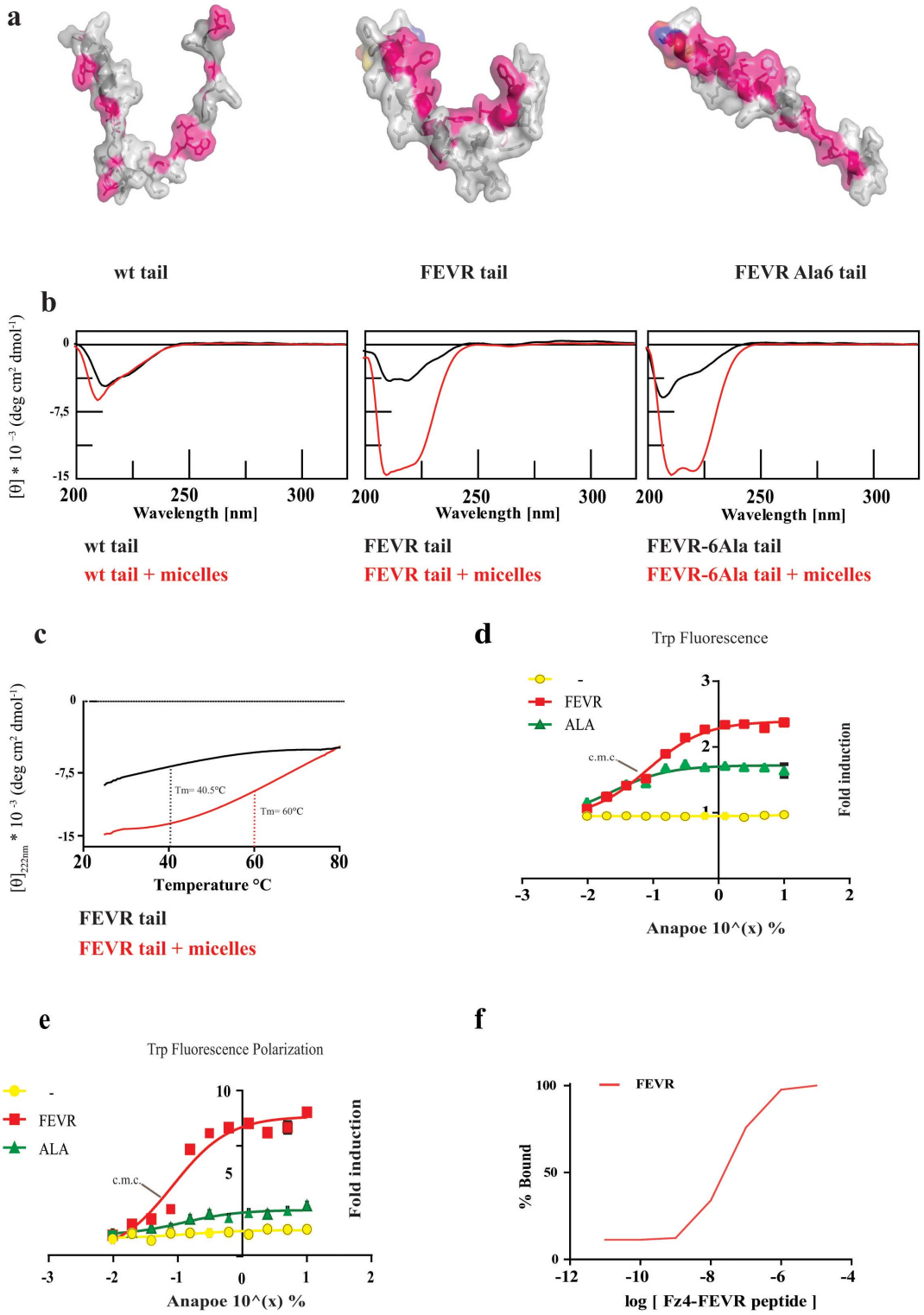

Figure 3 | **Fz4-FEVR tail has affinity for membranes.** (a) Surface representation of the structural predictions of Fz4, Fz4-FEVR and Fz4-FEVR-6Ala tails. Polar amino acids are indicated in gray, non polar in magenta; (b) CD spectra of the indicated peptides in the presence of micelles (red line). The spectra are superimposed with those recorded in the absence of micelles (black line) shown in Fig. 2d; (c) molar ellipticity at $\lambda = 222$ nm for Fz4-FEVR peptides in the presence (red line) or absence of micelles (black line) collected as a function of temperature. Melting temperatures (Tm) are indicated. (d) Trp fluorescence emission of Fz4-FEVR (red squares), Fz4-FEVR-6Ala (green triangles) tail peptides in the presence of increasing concentration of micellar agent. Fluorescence of the micellar agent is shown (yellow circles); (e) Trp fluorescence polarization of Fz4-FEVR and Fz4-FEVR-6Ala tail peptides in the presence of increasing concentration of micellar agent (shown as in c). c.m.c: critical micellar concentration for Anapoe (0.038% in water); (f) affinity of Fz4-FEVR tail peptide for rat liver microsomes.

ANAPOE-C10E6 micelles present physical properties (curvature, charge and shape) different from intracellular membranes, in particular ER membranes. Thus we measured the affinity of Fz4-FEVR peptide for microsomes obtained from rat liver. Hepatocites are enriched in ER membranes, so rat liver microsomes, obtained as previously described[33], were incubated with dilution of Fz4-FEVR peptide.

The unbound peptide was removed by centrifugation and the amount bound was detected after lysis by ELISA using a polyclonal antibody raised against Fz4-FEVR peptide. As shown in Fig. 3f we measured a Kd for microsomes of Fz4-FEVR peptide of around 50–100 nM confirming its affinity both for artificial micelles and for membranes.

Intracellular localization of Fz4-FEVR mutants. We envisaged that the new fold acquired by Fz4-FEVR tail and its affinity for membrane could explain Fz4-FEVR aggregation and ER retention. Therefore, mutants disturbing shape, hydrophobicity and charge of Fz4-FEVR tail were generated and their intracellular localization was analysed in transfected cells. In addition, the structural prediction of a series of double mutant was determined (Supplementary Fig. S2). Single substitution mutants are not considered sufficiently different from the Fz4-FEVR sequence by the structure prediction software's, so their effect on the fold of the tail is difficult to predict, on contrary they clearly affect either net charge, hydrophobicity of the tail or its ability to interact with membranes. All constructs were transiently expressed in Huh-7 cells and their localization was visualized by confocal immunofluorescence (Fig. 4). The percentage of mutant protein present on the cell surface was measured as described in the method section and reported in Supplementary Fig. S3. Truncation of the last seven residues of the tail (Fz4-FEVR 1-525) did not rescue the protein that localizes intracellularly in the ER. In contrast, truncation of the last 17 (Fz4-FEVR 1-515) and 23 (Fz4-FEVR 1-509) residues rescued the phenotype localizing both receptors on the PM and in the Golgi complex, thus suggesting proper intracellular trafficking when helix 2 alone, or together with the loop, is removed. The complete removal of the tail (Fz4-FEVR 1-498) did not rescue the phenotype, showing the need of a cytosolic tail for the folding of the receptor.

Interestingly, Fz4-FEVR-6Ala clearly localizes on PM and in the Golgi complex. A partial recovery was also visible for mutants with single or double substitutions in the region of the tail closer to the helix connecting loop (residues R_{519} to W_{524}). Alanine scanning in this region generated mutants (Fz4-FEVR-R_{519}A, Fz4-FEVR-K_{523}A and Fz4-FEVR-W_{524}A) with a rescued PM localization. Similar results were obtained when couple of residues was substituted in the same region (Fz4-FEVR-R_{519}A-E_{520}A, Fz4-FEVR-E_{520}A-E_{521}A, Fz4-FEVR-E_{521}A-R_{522}A, Fz4-FEVR-R_{522}A-K_{523}A and Fz4-FEVR-K_{523}A-W_{524}A). Single substitution performed outside the loop region did not rescue the localization of the receptor (Fz4-FEVR-W_{514}A). Double substitutions at the edge of the R_{519}-W_{524} region (Fz4-FEVR-K_{517}A-E_{518}A, Fz4-FEVR-G_{526}A-E_{527}A) did not rescue the PM localization. Taken together, these results strongly indicated that disturbing the mutant tail results in rescued Fz4-FEVR localization at the cell surface: either removal of helix 2 or of the loop or the substitution of residues in the loop region establishing lipid-protein interactions or affecting the tail curvature determine the export of the mutant receptor from the ER.

Effect of the Fz4-FEVR tail in a chimeric protein context. The results obtained raised the hypothesis that the Fz4-FEVR tail could be necessary and sufficient to induce misfolding and aggregation of transmembrane proteins. To test this hypothesis, chimeric constructs composed by ecto and transmembrane domains of the reporter molecule VSVG glycoprotein coded by the ts-045 mutant strain fused to the cytosolic tail either of Fz4-FEVR or of Fz4 wt were generated (Fig. 5). VSVG ts-045 is a temperature sensitive mutant of VSVG that localizes as misfolded monomer in the ER at non permissive temperature (40°C). When the permissive temperature (32°C) is re-established, the protein trimerizes and moves to the PM[34]. As shown in Fig. 5a, both VSVG-Fz4 wt tail and VSVG-Fz4-FEVR tail localized in the ER at non permissive temperature but only VSVG-Fz4 wt tail moved to the Golgi after the temperature shift. Analysed on a glycerol gradient, VSVG-Fz4 wt tail appears trimeric as expected[34] (Fig. 5b), while VSVG-Fz4-FEVR tail appears monomeric. Therefore, despite the different context, Fz4-FEVR tail induces ER retention of VSVG. However, differently from the effect triggered in its natural location, the Fz4-FEVR tail does not cause aggregation of VSVG but blocks it in a monomeric fold, not trimerization prone.

Discussion

Here we show that the mutation L501fsX533 induces a disorder-to-order structural transition in the cytosolic tail of the Fz4 receptor. To our knowledge, this is the first example of a transition occurring in an intrinsically disordered region of a mammalian protein experimentally analyzed[2,3]. The effect of such transition is deleterious for the folding of the Fz4 protein, its intracellular localization and activity.

The L501fsX533 frameshift mutation has a very unusual outcome. In the mutant coding sequence, the first stop codon is encountered 96 nucleotides after the deletion, thus creating a new reading frame coding for a different 32 amino acids long sequence (Fig. 2a). The ratio between charged, polar and non polar amino acids is almost unaltered between Fz wt and Fz4-FEVR tail sequence. In contrast, Trp and Phe residues are present in higher number in the Fz4-FEVR tail and increase its aromaticity, despite these amino acids rarely result from mutations due to the low degree of degeneration of their codons.

We prove that a synthetic peptide with the sequence of the Fz4-FEVR tail acquires a helical fold in solution. Specific negative peaks at around 208 and 222 nm in the CD spectrum confirmed its alpha helical fold (Fig. 2d). This is also indicated by structure prediction software's that suggest a boomerang shape formed by two consecutive helices connected by a loop (Fig. 2b). The first four amino acids of the wt tail were already shown to be part of a short juxtamembrane alpha helix[27], and are conserved in the mutant tail that is predicted to form a longer helix ending with the loop. The amino acids at the C terminal region in the wt tail have low helical propensity, especially Pro_{529}. In contrast, the absence of the Pro and the presence of Glu and Lys residues in the corresponding part of the Fz4-FEVR tail strongly favours the formation of the second helix.

The helix-loop-helix shape of the Fz4-FEVR tail would partially resemble the HA fusion peptide at the pH of fusion (Supplementary Figure S1). This aminoacidic region in the sequence of HA undergoes a conformational change when the viral protein is in the endosomal compartment and triggers a disorder-to-order transition dictating the acquisition of a boomerang shape similar to the one predicted for Fz4-FEVR tail at physiological pH. The hydrophobicity of this HA segment was shown to be essential for the insertion of the peptide in the bilayer of the host cell and small deviation of the angle of the boomerang was proven to abolish the fusogenic activity[29,30]. The two helices of the FEVR tail are not similarly hydrophobic but strongly amphipathic due to the presence on the same side of the helix of hydrophobic and aromatic residues (Val_{503}, Phe_{507}, Ile_{510}, Trp_{514} on the first helix and Leu_{525} and Trp_{529} on the other one)(Fig. 3a). In the wt tail the hydrophobicity is less anisotropic and thus the amphipathicity is absent.

We prove *in vitro* that, differently from the wt, the synthetic peptide of the Fz4-FEVR tail has affinity for lipids and for rat liver microsomes (Fig 3b–f). Absolute molar ellipticity, melting temperature, Trp fluorescence intensity and Trp fluorescence polarization of the Fz4-FEVR tail increase in the presence of *in vitro* formed micelles (Fig. 3b–e). The reduction of the tumbling speed of the peptide when immersed in the micelles is in favour of a high affinity

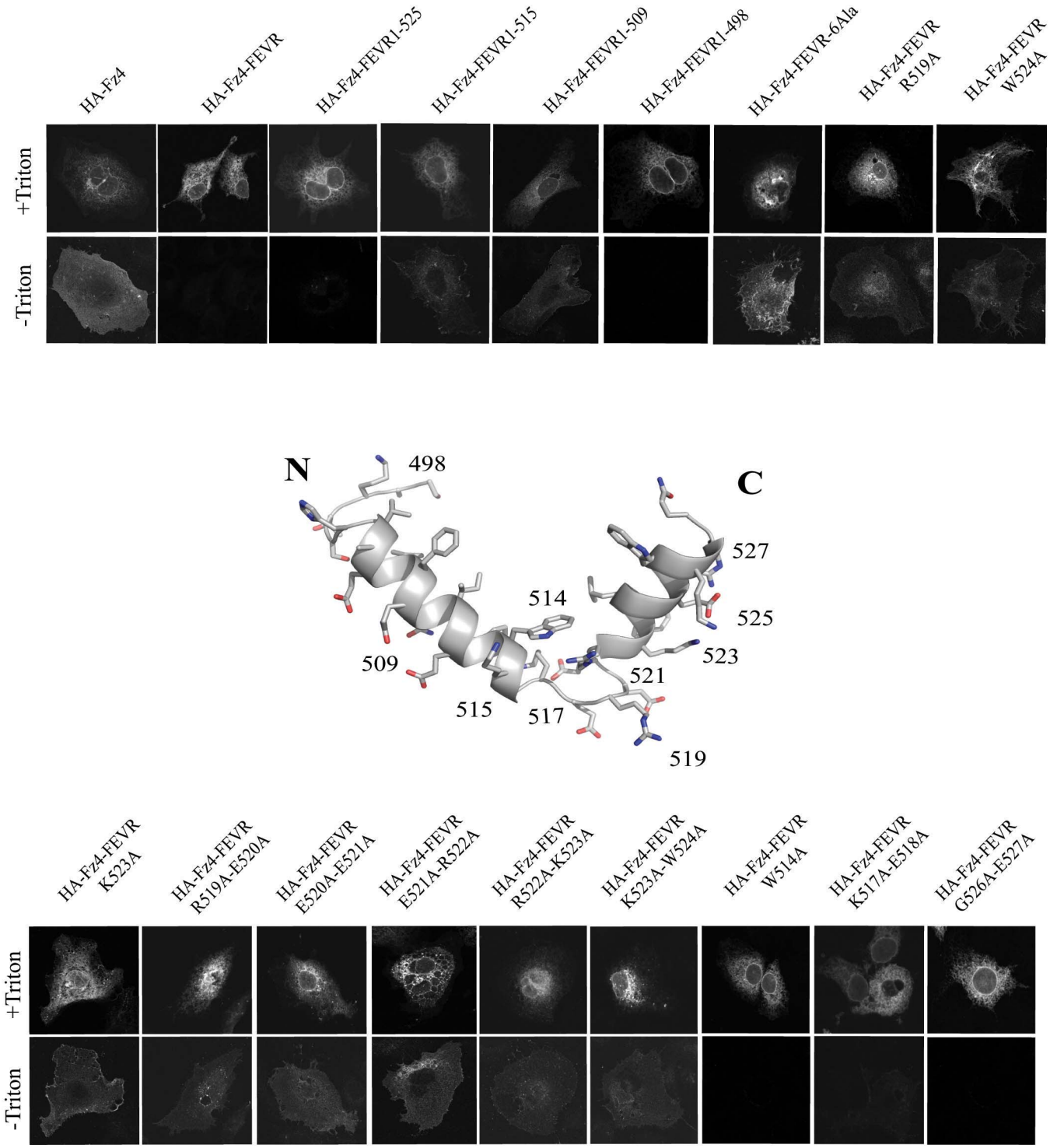

Figure 4 | Disturbing the fold of the tail induces the rescue of Fz4-FEVR to the PM. Surface (−Triton) and intracellular (+Triton) localization of Fz4, Fz4-FEVR and the indicated mutants transiently expressed in Huh-7 cells. Cartoon representation of Fz4-FEVR tail with side chains in ball and sticks showing the position of some of the mutated amino acids.

of the Fz4-FEVR peptide for the micelles. However, transmembrane segments prediction software (data not shown) exclude the possibility that the Fz4-FEVR tail would constitute an extra transmembrane segment of the receptor for the presence of highly charged Arg and Lys residues and support a peripheric interaction of this mutant tail with the membrane.

CD spectra indicate a structuring effect of the lipids on both Fz4-FEVR and Fz4-FEVR-6Ala tail peptides. Fz-FEVR-6Ala tail is more flexible (Fig. 2d) and get stabilized only by the presence of the micelles (Fig. 3b). The Fz4-FEVR tail helices are already partially stable (Fig. 2d) probably thanks to the loop that allows long distance aromatic contacts and Van der Waals interactions. For both the tails the lipids enforce the stability of the fold contributing with hydrophobic and polar interactions via their apolar fatty chains and their charged head, respectively (Fig. 3b).

The need of the helix-loop-helix conformation for inducing the phenotype of Fz4-FEVR receptor was confirmed in transfected cells. When a Fz4-FEVR mutant missing the second helix was expressed in

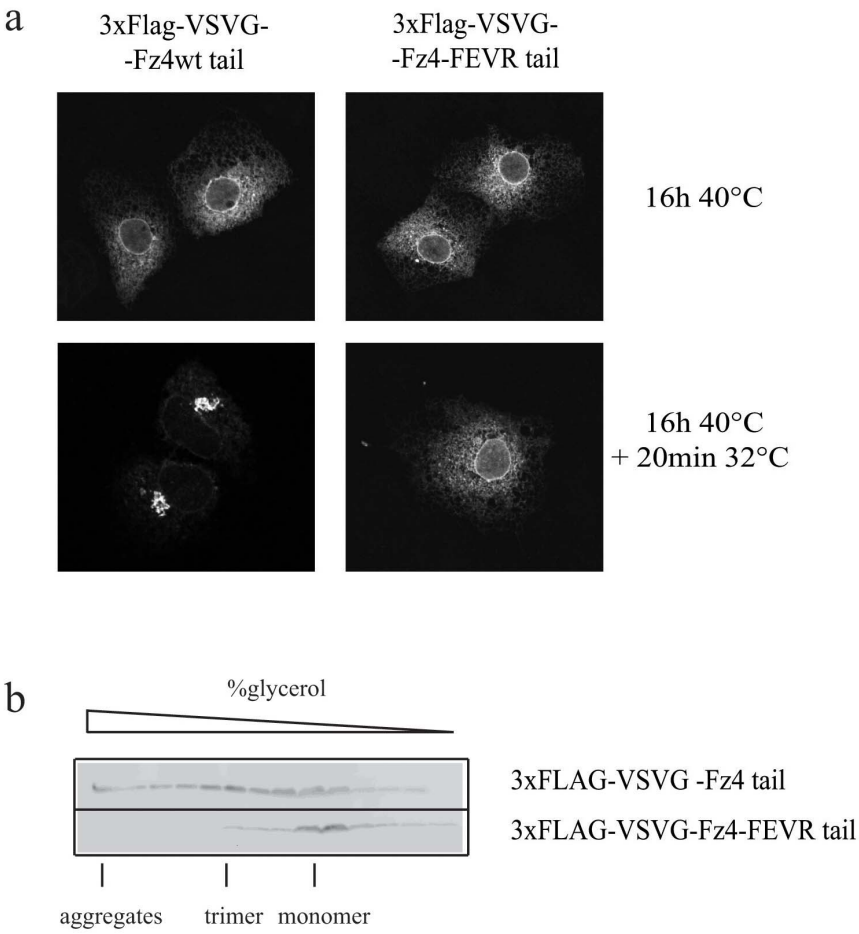

Figure 5 | Fz4-FEVR tail appended to the reporter molecule VSVG dictates ER retention of the chimera by misfolding. (a) Intracellular distribution of VSVG-Fz4 and VSVG-Fz4-FEVR tail transiently expressed in Huh-7 cells at not permissive and permissive temperature (40°C and 32°C, respectively); (b) Oligomeric state of VSVG-Fz4 tail and VSVG-Fz4-FEVR tail analyzed on glycerol gradient and SDS-PAGE analysis (the relevant parts of each of the two different gels are shown aligned; samples have been run under the same experimental conditions).

Huh-7 cells the receptor moved from the ER to the PM confirming the need of the second helical element (Fig. 4). The same rescue effect was seen for mutants missing also the loop (Fig. 4).

Six amino acids would form the kinked loop connecting the two helices in the Fz4-FEVR fold. It is not possible to unambiguously prove the presence and the geometry of the loop in cells but we proved that the sequence of the loop is essential for the Fz4-FEVR retention in the ER. When the Fz4-FEVR-6Ala mutant was expressed in cells, the wt phenotype was significantly rescued and a similar effect was seen for single or double substitutions in the loop region of the FEVR tail (Fig. 4 and supplementary Fig. S3). Different shapes and geometry are predicted for the tails of the mutants we tested (Supplementary Fig. S2). Moreover in most of them (especially Fz4-FEVR-6Ala) Alanine replaces residues with side chains known to establish interactions with the charged heads of the lipid bilayer (Arg, Lys and Glu) or with its hydrophobic part (Trp). The mutants predicted to be structurally divergent from Fz4-FEVR or with a different net charge of the tail localize on PM in transfected cells. This finding was already shown for HA fusion peptide where single mutations in its sequence alter the fusogenic activity and affects infectivity of the virus[29,30].

Our results strongly indicate that the interaction of the cytosolic tail of Fz4-FEVR with ER membranes reduces conformational freedom in the transmembrane segments of the Fz4 receptor leading to formation of incorrect disulphide bonds and aggregation (Fig. 6). Our hypothesis could also explain the strong ER retention induced by Fz4-FEVR tail in the context of the VSVG chimera. As shown by the sedimentation profile, VSVG-Fz4-FEVR tail is trapped in the ER in a pre-trimeric state (Fig. 5 a–b). The trimerization of VSVG is mostly dependent by the ectodomain and not by the cytosolic tail. Our results support a model where the orientation of the transmembrane of VSVG is altered by the cytosolic FEVR tail, and affects the proper interaction of the ectodomains of the glycoprotein probably by misalignment.

Our results underline the importance to experimentally analyze the effect of mutation also on short disordered regions of proteins and to consider the acquisition of a new fold as possible outcome of such mutations. This may be particularly relevant for the many receptors that have short and flexible cytosolic tails, such as the G protein coupled family members, and future work will be addressed to study if mutations in their cytosolic tails have an effect similar to the one we have observed on Fz4 folding. Specific antibodies, peptides or organic molecules directed against the mutated C-terminal tails could destabilize their fold and represent a therapeutic strategy to rescue the proper activity and localization of the receptors.

Methods

Chemicals. All culture reagents were obtained from Sigma-Aldrich (Milan, Italy). Solid chemicals and liquid reagents were obtained from E. Merck (Darmstadt, Germany), Farmitalia Carlo Erba (Milan, Italy), Serva Feinbiochemica (Heidelberg, Germany), Delchimica (Naples, Italy) and BDH (Poole, United Kingdom). The radiochemicals were obtained from Perkin Elmer (Bruxelles, Belgium). Protein A-Sepharose CL-4B and the ECL reagents were from Amersham Biosciences (Milan, Italy). Protease Inhibitor Cocktail was obtained from Roche (Milan, Italy). ANAPOE-$C_{10}E_6$ was obtained from Affymetrix (Santa Clara, California).

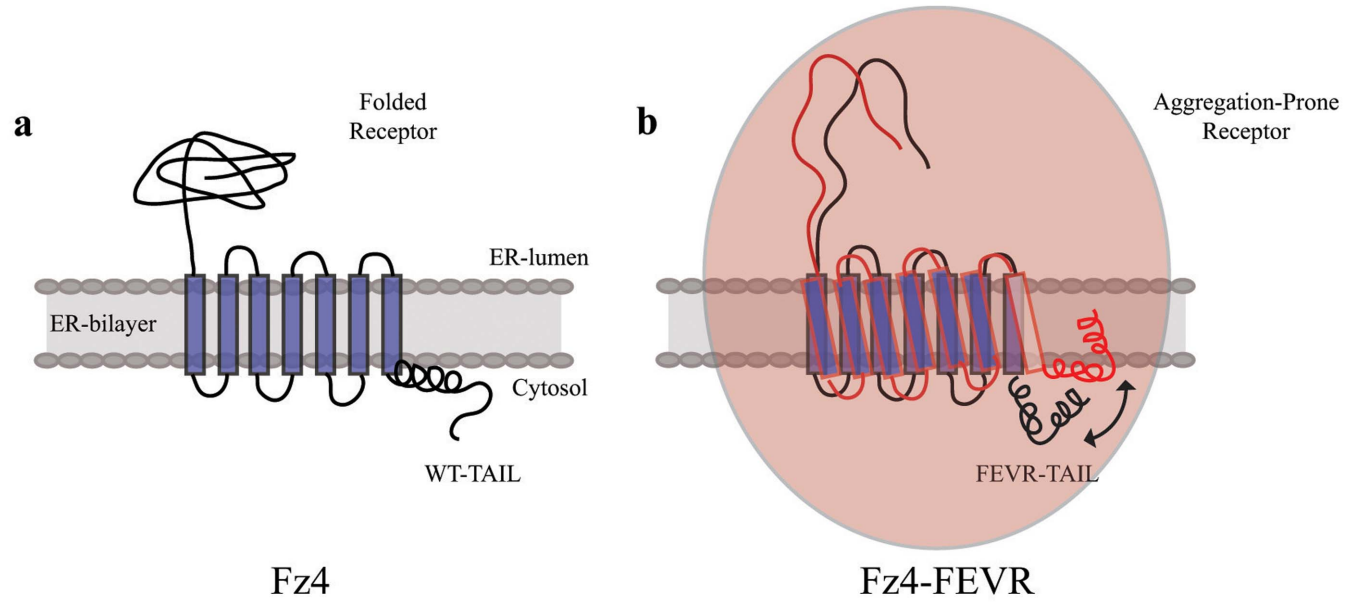

Figure 6 | Schematic cartoon showing the proposed orientation of Fz4 wt (a) and Fz4-FEVR tail (b) toward the lipid bilayer of the ER and the effect of the mutant tail on the folding of Fz4.

Antibodies. The following antibodies were used: mouse monoclonal anti-HA (Santa Cruz Biotechnology Inc.); rabbit polyclonal anti-HA (Sigma Aldrich); rabbit polyclonal anti-Calnexin (StressGene); Texas-Red-conjugated goat anti-mouse or rabbit IgG, FITC-conjugated goat anti-mouse or anti-rabbit IgG (Jackson Immunoresearch Laboratories, West Grove, PA, USA); mouse monoclonal anti-FLAG (Sigma Aldrich, Milan, Italy); mouse anti-GFP (Santa Cruz Biotechnology Inc.); rabbit polyclonal raised against Fz4-FEVR peptide was generated as previously described[22].

Peptides. Synthetic peptides corresponding to the sequence of: wt (CSAKTLHTWQKCSNRLVNSGKVKREKRGNGWVKPGKGSETVV), FEVR (CSAKTSHVAEVFQQIGEFWKGKEREERKWLGEAWKRQ), FEVR-6Ala (CSAKTSHVAEVFQQIGEFWKGKEAAAAAALGEAWKRQ) were purchased at GL Biochem (Shanghai).

The lyophilized powders were dissolved in deionized water at concentration of 5 mg/mL, to be then further diluted in the appropriate buffer. Concentration were determined with a NANODROP 2000 Spectrophotometer (Thermo Scientific), using extinction coefficient values of $\varepsilon_{wt} = 11125$, $\varepsilon_{FEVR} = 16500$, $\varepsilon_{6Ala} = 11000$, for the wt, FEVR and FEVR6Ala peptides, respectively.

Structure prediction. The structure prediction for Fz4 wt, FEVR and all the mutated tails were generated uploading the sequences to the Protein Model Portal (PMP)[35] server and using I-Tasser[36] as prediction tool. Cartoon representations, r.m.s. deviation, dihedral, planar angle calculations were done with Pymol Molecular Graphics System, (Version 1.5.0.4 Schrodinger, LLC). Disorder predictions were calculated using DisEMBL 1.5[37]. Predictions of Transmembrane regions were calculated with HMMTOP 2.0[38].

Circular dichroism. CD spectra were recorded in a Jasco J-710 CD Spectrophotometer. Peptides were diluted to the final concentration of 10^{-4} M in NaCl 150 mM and, where indicated, ANAPOE 2% was included. Data were recorded in the wavelength range 200 nm to 320 nm with a data pitch of 1 nm, in a continuous scanning mode at a speed of 50 nm/min. 4 seconds of response in standard sensitivity e 20 accumulations were used to generate the averaged spectra. Melting temperatures were determined measuring the molar ellipticity at 222 nm in a continuos mode raising the temperature of the sample from 25°C to 80°C (0.5°C per min). Spectra were averaged, baseline subtracted, and smoothed using Jasco Spectra Analyser and GraphPad 6.0.

Trp fluorescence quenching and polarization. Peptides, 10 μM (in Hepes 50 mM pH 8, 150 mM NaCl) were equilibrated with dilutions of the micellar agent ANAPOE $C_{10}E_6$ one hour before fluorescence measurement. Equilibrium fluorescence and Polarization measurement were monitored using a PheraStar fluorescence plate reader in 96 well plates. Peptides were excited at 280 nm, and emission intensity was monitored at 340 nm with an emission slit of 8 nm as already described[39]. Triplicates of the data were normalized and fitting to a sigmoidal dose-response curve was done in GraphPad.

Cell culture, transfection and immunofluorescence. Human HEK293T and Huh-7 cells were routinely grown at 37°C in Dulbecco's Modified Essential Medium (DMEM), containing 10% fetal bovine serum (FBS) and transfected by using FuGene 6.0 according to the manufacturer instruction. Indirect immunofluorescence was performed as previously described[33,40]. Single confocal images were acquired at 63× and 100× magnification on a LSM510 Zeiss Confocal Microscope (Carl Zeiss Jena, Germany).

To separately stain Fz4 proteins on either cell surface (extra) or intracellular membranes indirect immunofluorescence was performed as previously described[22]. Briefly cells were incubated after fixation with rabbit polyclonal anti-HA antibody, briefly fixed again, and then permeabilized and incubated with mouse monoclonal anti-HA antibody. Two distinct secondary antibodies allowed separate visualization of the two fractions. Then, in order to measure the ratio between levels of PM and intracellular Fz4 protein forms, the immunofluorescence intensity in the two channels was measured using NIH ImageJ Biophotonic programs. For each transfection, 20 cells were considered for quantification. The results are given as mean 6 s.d.

Pulse-chase & EndoH assay. HEK293T cells, transiently transfected with HA-Fz4 and HA-Fz4-FEVR, were starved for 30 minutes in DMEM without Cys and Met, containing 1% FBS. Cells were then pulse labelled for 20 minutes with S^{35}-CYS/MET (100 μCi/ml). After washing with PBS1X the cells were incubated for 2 and 4 hrs with DMEM 10% FBS containing cycloheximide (10 μg/mL). After washing with PBS1X, cells were lysed in B-Buffer (10 mM Tris-HCl pH 7.4, 150 mM NaCl pH 8.0, 1% Triton X-100) for 30 minutes on ice and HA-Fz4 and HA-Fz4-FEVR proteins were immonoprecipitated using a mouse monoclonal anti-HA antibody for 16 hrs at 4°C and Protein A-Sepharose beads (Pharmacia). After washing with lysis buffer, the immunoprecipitated proteins were treated with EndoH enzyme (New England BioLabs), according to the manufacturer's instructions, run on SDS-PAGE gels and analyzed by autoradiography.

Temperature shift assay. Huh-7 cells were cultured on coverslips and transfected with cDNA coding for VSVG constructs. 2 hours after transfection cells were first incubated at the non permessive temperature of 40°C for 16 hrs and then, when indicated, moved to the temperature of 32°C for 20 minutes. Coverslips were fixed in Formaldehyde 3,7% diluted in PBS before being processed by immunofluorescence and analyzed under the fluorescence microscope.

Velocity gradient. To the cell lisates, glycerol was added at the final concentration of 6% w/v, to be then loaded on the top of discontinuous 20 to the 40% glycerol gradients (5 ml final volume). After ultracentrifugation in a SW40.1 rotor at 45000 rpm of 16 hrs, 14 fractions were collected from the bottom of the gradient. All fractions were precipitated in 15% TCA for 2 hrs at 4°C. After 30 minutes of centrifugation, the pellets were washed two times with ice cold aceton, solubilized in Laemmli Buffer run on a SDS-PAGE and analysed by immunoblotting.

Affinity of Fz4-FEVR tail peptide for rat liver microsomes. Rat liver microsomes were prepared as previously described[33]. 15 to 30 μg of membranes were incubated for 1 hour at 4°C with Fz4-FEVR peptide diluted in PBS (peptide concentration ranging from 10 μM to 1 nM). Bound peptides were collected by centrifugation of microsomes at 13.200 rpm for 10 minutes at 4°C. After being washed twice in cold PBS microsomes were precipitated in 90% cold acetone at −20°C for 12 hours and the protein fraction sedimented by centrifugation at 14.000 rpm for 30 minutes. The

dried pellets were resuspended in Tris 50 mM pH 8.0, NaCl 150 mM and absorbed on ELISA plates for 12 hours. Elisa wells were blocked with 3% BSA solution. Primary antibody raised against FZ4-FEVR tail was used to detect Fz4-FEVR peptide (dilution 1 : 500 in PBS 0.3% BSA, incubation time 3 hours). Secondary AP-conjugated antibody (SIGMA) was used 1 : 2000 for 3 hours. AP substrate PNPP (Pierce) was used following manufacturer procedure.

1. Yue, P., Li, Z. & Moult, J. Loss of protein structure stability as a major causative factor in monogenic disease. *J. Mol. Biol.* **353**, 459–473 (2005).
2. Vacic, V. *et al.* Disease-Associated Mutations Disrupt Functionally Important Regions of Intrinsic Protein Disorder. *PLoS Comput. Biol.* **8**, e1002709 (2012).
3. Vacic, V. & Iakoucheva, L. M. Disease mutations in disordered regions-exception to the rule? *Mol. Biosyst.* **8**, 27–32 (2012).
4. Dinkel, H. *et al.* ELM–the database of eukaryotic linear motifs. *Nucleic Acids Res.* **40**, D242–251 (2012).
5. Fuxreiter, M., Tompa, P. & Simon, I. Local structural disorder imparts plasticity on linear motifs. *Bioinformatics* **23**, 950–956 (2007).
6. Dyson, H. J. & Wright, P. E. Intrinsically unstructured proteins and their functions. *Nat Rev. Mol. Cell Biol.* **6**, 197–208 (2005).
7. Tompa, P., Szasz, C. & Buday, L. Structural disorder throws new light on moonlighting. *Trends Biochem. Sci.* **30**, 484–9 (2005).
8. Radivojac, P. *et al.* Intrinsic disorder and functional proteomics. *Biophys. J.* **92**, 1439–56 (2007).
9. Dyson, H. J. & Wright, P. E. Coupling of folding and binding for unstructured proteins. *Curr. Opin. Struct. Biol.* **12**, 54–60 (2002).
10. Minde, D. P., Anvarian, Z., Rudiger, S. G. & Maurice, M. M. Messing up disorder: how do missense mutations in the tumor suppressor protein APC lead to cancer? *Mol. Cancer* **10**, 101 (2011).
11. Schulte, G. & Bryja, V. The Frizzled family of unconventional G-protein-coupled receptors. *Trends Pharmacol. Sci.* **28**, 518–25 (2007).
12. Wang, C. *et al.* Structure of the human smoothened receptor bound to an antitumour agent. *Nature* **497**, 338–43 (2013).
13. Wang, H. Y., Liu, T. & Malbon, C. C. Structure-function analysis of Frizzleds. *Cell Signal.* **18**, 934–41 (2006).
14. Chen, W. *et al.* Dishevelled 2 recruits beta-arrestin 2 to mediate Wnt5A-stimulated endocytosis of Frizzled 4. *Science* **301**, 1391–4 (2003).
15. Wong, H. C. *et al.* Structural basis of the recognition of the dishevelled DEP domain in the Wnt signaling pathway. *Nat. Struct. Biol.* **7**, 1178–84 (2000).
16. Umbhauer, M. *et al.* The C-terminal cytoplasmic Lys-thr-X-X-X-Trp motif in frizzled receptors mediates Wnt/beta-catenin signalling. *EMBO J.* **19**, 4944–54 (2000).
17. Robitaille, J. *et al.* Mutant frizzled-4 disrupts retinal angiogenesis in familial exudative vitreoretinopathy. *Nat. Genet.* **32**, 326–30 (2002).
18. Kaykas, A. *et al.* Mutant Frizzled 4 associated with vitreoretinopathy traps wild-type Frizzled in the endoplasmic reticulum by oligomerization. *Nat. Cell Biol.* **6**, 52–8 (2004).
19. Xu, Q. *et al.* Vascular development in the retina and inner ear: control by Norrin and Frizzled-4, a high-affinity ligand-receptor pair. *Cell* **116**, 883–95 (2004).
20. Wang, Y. *et al.* Norrin/Frizzled4 signaling in retinal vascular development and blood brain barrier plasticity. *Cell* **151**, 1332–44 (2012).
21. Han, X., Bushweller, J. H., Cafiso, D. S. & Tamm, L. K. Membrane structure and fusion-triggering conformational change of the fusion domain from influenza hemagglutinin. *Nat. Struct. Biol.* **8**, 715–20 (2001).
22. D'Agostino, M. *et al.* The cytosolic chaperone alpha-Crystallin B rescues appropriate folding and compartmentalization of misfolded multispan transmembrane proteins. *J. Cell Sci.* (2013) Epub ahead of print.
23. O'Brien, J. R. *et al.* Insight into the mechanism of the B12-independent glycerol dehydratase from Clostridium butyricum: preliminary biochemical and structural characterization. *Biochemistry* **43**, 4635–45 (2004).
24. Gangelhoff, T. A., Mungalachetty, P. S., Nix, J. C. & Churchill, M. E. Structural analysis and DNA binding of the HMG domains of the human mitochondrial transcription factor A. *Nucleic Acids Res.* **37**, 3153–64 (2009).
25. Remenyi, A. *et al.* Crystal structure of a POU/HMG/DNA ternary complex suggests differential assembly of Oct4 and Sox2 on two enhancers. *Genes Dev.* **17**, 2048–59 (2003).
26. Sharma, Y. *et al.* Modified helix-loop-helix motifs of calmodulin--The influence of the exchange of helical regions on calcium-binding affinity. *Eur. J. Biochem.* **243**, 42–8 (1997).
27. Punchihewa, C., Ferreira, A. M., Cassell, R., Rodrigues, P. & Fujii, N. Sequence requirement and subtype specificity in the high-affinity interaction between human frizzled and dishevelled proteins. *Protein Sci.* **18**, 994–1002 (2009).
28. Kelly, S. M., Jess, T. J. & Price, N. C. How to study proteins by circular dichroism. *Biochem. Biophys. Acta* **1751**, 119–39 (2005).
29. Lai, A. L., Park, H., White, J. M. & Tamm, L. K. Fusion peptide of influenza hemagglutinin requires a fixed angle boomerang structure for activity. *J. Biol. Chem.* **281**, 5760–70 (2006).
30. Lai, A. L. & Tamm, L. K. Locking the kink in the influenza hemagglutinin fusion domain structure. *J. Biol. Chem.* **282**, 23946–56 (2007).
31. Helenius, A., McCaslin, D. R., Fries, E. & Tanford, C. Properties of detergents. *Methods Enzymol.* **56**, 734–49 (1979).
32. Heidebrecht, T. *et al.* Binding of the J-binding protein to DNA containing glucosylated hmU (base J) or 5-hmC: evidence for a rapid conformational change upon DNA binding. *J. Am. Chem. Soc.* **134**, 13357–65 (2012).
33. Stornaiuolo, M. *et al.* KDEL and KKXX retrieval signals appended to the same reporter protein determine different trafficking between endoplasmic reticulum, intermediate compartment, and Golgi complex. *Mol. Biol. Cell* **14**, 889–902 (2003).
34. Doms, R. W., Keller, D. S., Helenius, A. & Balch, W. E. Role for adenosine triphosphate in regulating the assembly and transport of vesicular stomatitis virus G protein trimers. *J. Cell. Biol.* **105**, 1957–69 (1987).
35. Arnold, K. *et al.* The Protein Model Portal. *J. Struct. Funct. Genomics* **10**, 1–8 (2009).
36. Zhang, Y. I-TASSER server for protein 3D structure prediction. *BMC Bioinformatics* **9**, 40 (2008).
37. Linding, R. *et al.* Protein disorder prediction: implications for structural proteomics. *Structure* **11**, 1453–9 (2003).
38. Tusnady, G. E. & Simon, I. Principles governing amino acid composition of integral membrane proteins: application to topology prediction. *J. Mol. Biol.* **283**, 489–506 (1998).
39. Stornaiuolo, M. *et al.* Assembly of a triple pi-stack of ligands in the binding site of Aplysia Californica acetylcholine binding protein (AChBP). *Nat. Comm.* **4**, (2013).
40. Radner, S. *et al.* Transient transfection coupled to baculovirus infection for rapid protein expression screening in insect cells. *J. Struct. Biol.* **179**, 46–55 (2012).

Acknowledgements

This work was supported in part by Telethon grants (GGP09029 to SB). We thank TIGEM Advanced Microscopy and Imaging Core for microscopy support. We thank Alex Fish, Jens Hausmann, Luigi Vitagliano and Vittorio Limongelli for fruitful discussions.

Author contributions

The experimental work was performed by V.L., with contribution from M.S. for the structure prediction, Fluorescence measurements and peptide conformational analysis, from M.S. and G.O. for CD measurements, and from M.G.C., M.M. and M.d.A. for cell culturing and the IF image aquisition. M.S., S.B. and V.L. planned the work and analyzed the results. The paper was written by M.S., S.B. and V.L. with assistance from the other authors.

Additional information

Supplementary information accompanies this paper at http://www.nature.com/scientificreports

Competing financial interests: The authors declare no competing financial interests.

How to cite this article: Lemma, V. *et al.* A disorder-to-order structural transition in the COOH-tail of Fz4 determines misfolding of the L501fsX533-Fz4 mutant. *Sci. Rep.* **3**, 2659; DOI:10.1038/srep02659 (2013).